Crystal seeded growth of pH-responsive metal-organic framework for enhancing encapsulation, stability and bioactivity of hydrophobicity compounds

by Liu, Z., Wu, Q., He, J., Vriesekoop, F. and Liang, H.

DOI: https://doi.org/10.1021/acsbiomaterials.9b01070

Liu, Z., Wu, Q., He, J., Vriesekoop, F. and Liang, H. 2019. Crystal-Seeded Growth of pH-Responsive Metal–Organic Frameworks for Enhancing Encapsulation, Stability, and Bioactivity of Hydrophobicity Compounds. *ACS Biomaterials Science & Engineering*, *5*(12), pp.6581-6589.

Crystal seeded growth of pH-responsive metal-organic framework for enhancing encapsulation, stability and bioactivity of hydrophobicity compounds

Zexun Liu, [†] Qiao Wu, [†] Jie He, [†] Frank Vriesekoop, [‡,] * and Hao Liang[†,] *

[†] State Key Laboratory of Chemical Resource Engineering, Beijing University of Chemical Technology, Beijing100029, P. R. China

[‡] Department of Food Technology and Innovation, Harper Adams University, Newport TF10 8NB, Shropshire, England

KEYWORDS: ZIF-L, microcrystal of curcumin, pH-responsive, drug delivery, cancer treatment

ABSTRACT: Zeolitic imidazolate framework-L (ZIF-L) could effectively improve the stability, controlled release and anticancer activity of natural hydrophobicity drugs in drug delivery systems (DDS). A simple and universal strategy was developed to prepare the curcumin-loaded ZIF-L (CCM@ZIF-L) by antisolvent coprecipitation method, which was different from the traditional approaches. The microcrystal molecules of curcumin were used as the core of ZIF-L growth to

form CCM@ZIF-L, which has a very high drug encapsulation efficiency of 98.21% and a regular leaf or cruciate flower-like structure. The formation of CCM@ZIF-L with distinct composite structure was supported by SEM, TEM, FTIR, PXRD and zeta-potential. Due to the protective effect of ZIF-L, CCM@ZIF-L exhibited excellent stability and about a 5-fold increase in temperature stability over free curcumin. CCM@ZIF-L exhibited controlled drug release behavior in simulated *in vitro* tumor microenvironments (almost 81.2 % drug release over a period of 72 h). Furthermore, confocal laser-scanning microscopy (CLSM) results and cytotoxicity experiments confirmed that the encapsulated curcumin showed a significant improvement in cellular uptake and anticancer activity against A549 cancer cells. Moreover, the curcumin encapsulated in ZIF-L exhibited remarkable cellular antioxidant activity based on MGC-803 cell models. This work presents a novel approach to solve the drug loading problem employing ZIF-L, and exhibits enormous potential of ZIF-L as an effective DDS in cancer treatments.

1. Introduction

With the continuing deterioration of the global environment and changes in people's lifestyle, a wide range of cancers have become a persistent predicament with regards to human health.[1-2] A growing number of natural bioactive molecules are considered promising candidates for cancer treatment, because they showed less toxicity to non-cancerous cells compared to more conventional synthetic compounds.[3-4] However, direct administration of some natural hydrophobic drugs suffer from some intrinsic limitations, including poor solubility, compromised physiological stability and low bioavailability. In response, a variety of drug delivery systems (DDS) such as polymer nanoparticles, liposomes, and metal organic frameworks (MOFs) have been realized to address some of these limitations by improving dispersibility in aqueous media, stabilizing the drug through encapsulation and facilitating enhanced cellular uptake.[5-16]

MOFs are constructed using organic ligands and metal ions and exhibit unique features such as uniform shapes and pore sizes, improved bioavailability and controlled drug release.[17-22],[23] There are two tactics that have been commonly pursued to achieve effective drug delivery employing MOFs.[24-25] In the first method, the drug is absorbed by pre-synthesized MOFs. This tactic is appropriate for drugs that are relatively small in size.[26] However, this approach can cause significant drug leakage during the final washing step, because the pores of the pre-synthesised MOFs are too large relative to the drug to be carried. This can result in a low encapsulation efficiency and 'burst-release' behavior.[25] An alternative tactic is to have the drug in question encapsulated *in-situ* during the assembly of MOFs.[27-33] Employing this tactic could accomplish the loading of drugs of various sizes into MOFs regardless of pore size, avoiding excessive drug leakage through 'burst-release' prior to the degradation of MOFs. Nonetheless a strong interaction between MOFs and drugs is essential in order to achieve successful *in-situ* encapsulation, which

is typically limited to drugs with specific functional groups (-COOH, -SO_3H, C=O, etc.) or opposite charge. It is worth noting that a majority of the drug loading processes employing MOFs are carried out in organic solvents.[27-31]

Zeolitic Imidazolate Framework L (ZIF-L), is formed by Zn^{2+} and 2-methylimidazole (2-MIM) in an aqueous solution at a relatively low ratio of 2-MIM/Zn^{2+}.[34] ZIF-L has a pore structure similar to ZIF-8, with long-term physical stability, resistance to thermal degradation, and high loading efficiency and has been extensively researched for applications such as: gas separation and water treatment.[34-35] However, few researches have demonstrated that ZIF-L could be a potential candidate for drug delivery systems.

We developed a simple and straightforward methodology for the encapsulation of hydrophobic drugs in ZIF-L using an antisolvent co-precipitation method under mild conditions. Curcumin (CCM) was chosen as a model drug in this study because of its hydrophobicity, low bioavailability and rapid degradation under physiological pH conditions.[40] As a natural bioactive compound, curcumin has extensive therapeutic uses, such as antitumor, antioxidation and antibacterial applications.[36-39] We used crystal seeded growth of ZIF-L MOFs in aqueous media to achieve the drug (i.e. curcumin) loading process. The microcrystal particles of curcumin were chosen as the core of ZIF-L growth. The ZIF-L *in-situ* self-assembly based on microcrystal particles of curcumin was achieved by a co-precipitation method to obtain the curcumin-loaded ZIF-L (CCM@ZIF-L). As shown in **Scheme 1**, this drug delivery system was assembled by *in-situ* encapsulation, which synchronized the process of ZIF-L synthesis and drug loading. This new designed CCM@ZIF-L DDS had the following advantages: (1) The use of microcrystal particles overcome the limitations of traditional drug loading with MOFs, achieving an ultrahigh drug encapsulation efficiency of 98.2 %. (2) This novel encapsulation approach enhanced the

83 physiological stability, cellular uptake and targeted anticancer activity of the drug. (3) Controlled
84 drug release was observed in tumor cells, due to pH-responsive degradation of ZIF-L.
85 Consequently, this study offers an effective approach to broaden the applications of ZIFs for
86 anticancer therapy and exhibited great potential of ZIF-L as a drug carrier platform.

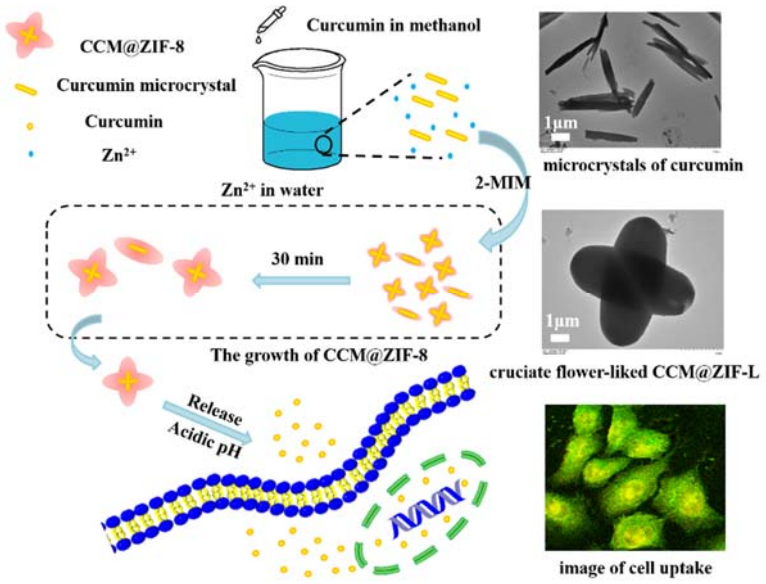

87

88 **Scheme 1.** Schematic outline for the synthesis and assembly of CCM@ZIF-L and its pH-
89 responsive drug release mechanism.

90 2. Experimental section

91 2.1 Materials and Cell Culture

92 Curcumin (reagent grade 98 %), 2-Methylimidazole (2-MIM, reagent grade 98 %), zinc
93 nitrate hexahydrate ($Zn(NO_3)_2 \cdot 6H_2O$, analytical grade), 2,2-Diphenyl-1-picrylhydrazyl radical
94 (DPPH, reagent grade 96 %), tyrosinase (25 KU, from mushroom) and 3, 4-dihydroxy-l-
95 phenylalanine (L-DOPA, reagent grade 99 %) were obtained from Aladdin Inc. (Shanghai, China).
96 2,2-azobis (2-amidinopropane) dihydrochloride (ABAP) and 2,7-dichlorodi-hydrofluorescein

97 diacetate (DCFH-DA) were obtained from Sigma-Aldrich (St. Louis, MO, USA). Propidium
98 Iodide (PI) and the Cell Counting Kit-8 (CCK-8) were obtained from Dojindo Laboratories
99 (Kumamoto, Japan). RPMI-1640 culture media, trypsin-EDTA (0.05% (w/v)), fetal bovine serum
100 (FBS), penicillin and streptomycin were purchased from Gibco (NY, USA). A549 cells (human
101 alveolar basal epithelial cells) and MGC-803 (human gastric cancer cell) were obtained from the
102 Cell Resource Center, Peking Union Medical College, and cultured in RPMI-1640 media
103 supplemented with 10 % FBS and 1% (w/v) penicillin and streptomycin in a 5 % CO_2 atmosphere,
104 at 37 ℃. All other chemicals were of analytical grade and purchased from Beijing Chemical
105 Works (Beijing, China), and were applied without further purification.

106 **2.2 HPLC analysis**

107 A curcumin stock solution was prepared by dissolving 5 mg of curcumin in methanol in a 100
108 mL brown volumetric flask, which was then further diluted into various standard solutions at 1, 2,
109 3, 4, 5 μg/mL with methanol. Curcumin was analyzed by HPLC (LC-20A, Japan), using a Venusil
110 XBP C18 column (4.6 × 250 mm, 5 μm) with a mobile phase made of 0.5 % acetic acid (A) and
111 acetonitrile (B) with an isocratic elution program at 44:56 for solutions A and B respectively. The
112 flow rate was 1.0 mL/min, and the column temperature maintained isothermally at 35 °C.
113 Curcumin was detected using a UV-vis detector at 428 nm. As shown in **Figure S1**, a good
114 linearity was observed over the range of 1-5 μg/mL ($R^2 = 0.9999$).

115

116 **2.3 Synthesis of Curcumin loaded Zeolitic Imidazolate Framework-L (CCM@ZIF-L)**

117 Due to its highly hydrophobic nature, we produced a curcumin stock solution by dissolving
118 20 mg of curcumin in 10 mL of methanol. Solutions of $Zn(NO_3)_2 \cdot 6H_2O$ (30 mg/mL) and 2-MIM
119 (66 mg/mL) were prepared using deionized water. In order to create microcrystal molecules of

curcumin in an aqueous solution, 10 mL of the curcumin stock solution was added into 50 mL of the $Zn(NO_3)_2$ solution under vigorous stirring for 5 min. The vigorously stirred mixture was then drop-wise added into the 2-MIM aqueous solution (50 mL) under continuous stirring for 30 minutes. The reaction mixture was centrifuged, and the brick-red precipitate (CCM@ZIF-L) was washed thoroughly thrice with deionized water. The supernatant was collected to determine the drug loading efficiency (DLE). The DLE of CCM@ZIF-L was calculated according to the following equation (1).

Do I get it right that what you really calculated was:

$$\text{DLE}(\%)=\frac{\text{total amount of curcumin added - curcumin in supernatant}}{\text{total amount of curcumin added}}\times 100\%$$

$$\text{DLE}(\%)=\frac{\text{amount of curcumin retained in ZIF-L}}{\text{total amount of curcumin added}}\times 100\%$$

The synthesized CCM@ZIF-L was dispersed in deionized water and immediately analysed by scanning electron microscopy (SEM), transmission electron microscopy (TEM), confocal laser scanning microscopy (CLSM), and dynamic light scattering (DLS). The CCM@ZIF-L precipitate required for other analyses was freeze-dried prior to use. Furthermore, a pure ZIF-L was synthesized in the same manner as described above for comparison. All operations were conducted at room temperature.

2.4 Characterization

Fluorescence spectra and UV−vis absorption spectra were recorded using a RF-1501 spectrofluorometer (Shimadzu, Kyoto, Japan) and a UV-2450 spectrophotometer (Shimadzu,

Kyoto, Japan), respectively. The morphology of CCM@ZIF-L was characterized employing a Hitachi HT7700 TEM (Hitachi, Tokyo, Japan), a Hitachi S-4700 SEM (Hitachi, Tokyo, Japan), and a Leica SP8 CLSM (Leica, Wetzlar, Germany). In order to determine the Zeta potentials of CCM@ZIF-L and ZIF-L, Dynamic Light Scattering (DLS) was carried out employing a Nano-ZS 2000 (Malvern Instruments, Malvern, UK). FTIR (Fourier-transform infrared) spectra were performed on a Nicolet 6700 FTIR spectrometer (Waltham, MA, USA) equipped with a DLaTGS detector. The samples for FTIR analysis were prepared with KBr and compressed into tablets before analysis. An X-ray diffractometer (Bruker XRD, D8 ADVANCE) (Karlsruhe, Germany) equipped with a copper target X-ray tube set at 40 kV and 40 mA, employing Cu Kα radiation was used to obtain powder X-ray diffraction patterns (PXRD). All PXRD analysis were done in the 2θ angle range between 5˚ and 30˚ with a scan rate of 10˚ /min and a step size of 0.02˚.

2.5 *In vitro* stability

The stability of free curcumin and CCM@ZIF-L in phosphate buffer saline (PBS, 0.02 M) at different temperatures (25 °C, 45 °C, 65 °C or 85 °C), pH (5.4, 6.4, 7.4 or 8.4) and light conditions (dark, light or UV light at 254 nm) was analysed by monitoring the changes in absorbance at 428 nm. The CCM@ZIF-L solutions were prepared by dispersing the previously freeze-dried samples in deionized water while being stirred. The free curcumin solution was prepared by dispersing 1 mL of the curcumin stock solution into 50 mL of deionized water (final concentration: 1 mg/L curcumin in 2% (v/v) methanol) under the same conditions as CCM@ZIF-L. The curcumin concentration encapsulated in CCM@ZIF-L was evaluated by HPLC after disintegrated of CCM@ZIF-L in 1 M hydrochloride.

2.6 *In vitro* Drug Release

The *in vitro* pH-responsive release behavior of CCM@ZIF-L was investigated by a previously described method, but adjusted for curcumin.[41] Briefly, 10 mg of CCM@ZIF-L were dispersed into 50 mL of PBS (0.02 M, pH=7.4 or 5.0), at 37 °C while being gently shaken. Due to the poor solubility of curcumin in water, the dispersive stability of the released curcumin was significantly improved by adding Tween-80 (1.0 wt%) into PBS. The relative percentage of the accumulative release of curcumin was calculated as a function of incubation time. All operations were performed in triplicate.

2.7 Biocompatibility test

The biocompatibility of ZIF-L on basal lung cancer cells (A549 cell line) was examined using a cell counting kit (CCK-8).[42] A549 cells were seeded in 96-well plates at a density of 4000 cells per well and incubated in the RPMI-1640 culture medium for 12 h at 37 °C. The cells were exposed to ZIF-L (0-100 μg/mL) for 72 h at 37 °C, following which the spent medium was replaced by fresh RPMI-1640 medium. Then ten μL CCK-8 was added and incubated for another 1 h at 37 °C. A microplate reader was used to measure the absorbance of each well at 450 nm. The cell viability was calculated according to the following equation (2).

$$\text{Cell viability (\%)} = \frac{A_{treated}}{A_{control}} \times 100\%$$

Where the culture media treated with DMSO represented the control group. The mean and standard deviation from three-well replicates were calculated.

2.8 *In vitro* cytotoxicity study

A cytotoxicity assay was conducted to investigate the *in vitro* anticancer ability of both free curcumin and CCM@ZIF-L on A549 cells.[24, 43] A549 cells were seeded into 96-well plates with a cell loading of 4000 per well and then incubated in RPMI-1640 culture medium for 12 h at 37 °C. After that, fresh medium containing various concentrations of free curcumin or CCM@ZIF-L was used to replace the initial culture medium at an equivalent concentration of curcumin for all samples varying from 1 to 5 μg/mL and incubated for 72 h at 37 °C, after which the spent culture medium was replaced with fresh medium containing 10 μL of CCK-8. The microtiter plates were then incubated for another 1 h at 37 °C before the absorbance was read at 450 nm and cell viability was calculated using the equation above (2).

2.9 Cellular uptake study

Cellular uptake of curcumin from CCM@ZIF-L into A549 cells was determined employing CLSM according to a previously described method, adjusted for curcumin.[44] A549 cells (5×10^4 cells per well in Laser confocal dishes) were incubated in RPMI-1640 culture medium and allowed to adhere for 12 h after which the culture medium was replaced by fresh medium containing free curcumin or CCM@ZIF-L, containing a final curcumin concentration equivalent to 5 μg/mL. The cells were cultured for 4 h and then washed thrice with fresh PBS. After that, the cells were fixed with 4 % formaldehyde (800 μL per well) for 30 min at room temperature and washed again three times with PBS. Subsequently, the fluorescent dye PI (200 μL) was used to stain the cells for 15 min in the absence of light. Prior to imaging, all wells were washed thrice with PBS. Images were captured by exciting PI at 488 nm and curcumin at 442 nm, and measuring the emitted light at 630 nm and 475 nm for PI and curcumin respectively.

209 **2.10 Cellular Antioxidant Activity**

210 We used a previously described approach to investigate the antioxidant activity of free
211 curcumin and CCM@ZIF-L in the living cells.[45-46] This method used an oxidized cell model
212 employing ABAP, which generates intracellular hydrogen peroxide free radicals. DCFH-DA is
213 readily internalized by cells and converted into non-fluorescent DCFH by intracellular esterases
214 after which DCFH can then be oxidized to form fluorescent DCF. If cells were treated with
215 antioxidants (curcumin) from the outset, the oxidation of DCFH into DCF could be prevented. The
216 antioxidant activity of added antioxidants could be ascertained through a reduction in DCF
217 fluorescence.

218 For our study the human gastric cancer cell line MGC-803 was chosen to evaluate the cellular
219 antioxidant capacity (CAA) as described elsewhere.[47] Cells (4000 cells per well) were seeded into
220 96-well microtitre plates and incubated in RPMI-1640 culture medium for 24 h. After that, the
221 spent culture medium was discarded and replaced by 100 μL fresh medium containing curcumin,
222 or CCM@ZIF-L, or ZIF-L (equivalent concentration of curcumin as 2 μg/mL and/or the same
223 amount of ZIF-L) and incubated for a further 24 h. After 24 h the cells were washed thrice with
224 PBS and replaced with fresh medium containing DCFH-DA (25 μM, 100 μL) and incubated for 1
225 h. Then, the wells were washed three times with PBS, before being treated with ABAP (600 μM,
226 100 μL) in fresh medium. The fluorescent intensity was measured at an excitation wavelength and
227 an emission wavelength of 485 nm and 355 nm respectively, every 5 minutes for 1 h. Negative
228 controls were treated with DCFH-DA and ABAP without the addition of curcumin, while blank
229 controls were treated with DCFH-DA only. The resultant time-fluorescence intensity curve was
230 integrated to obtain the area, and then the CAA units could be calculated according to the following
231 equation (3).

232 $$CAA=100-\left(\frac{(\int A_s-\int A_b)}{(\int A_c-\int A_b)}\right)\times 100$$

233 $\int A_s$ represents the integral area of the fluorescence value-time curve after adding different
234 concentrations of antioxidant.

235 $\int A_c$ represents the integral area of the fluorescence value-time curve associated with the
236 experimental 'control'

237 $\int A_b$ represents the integral area of the fluorescence value-time curve associated with the
238 experimental 'blank'.

239 The mean and standard deviation from three-well replicates were calculated.

240

241 **2.11 Tyrosinase inhibitory activity**

242 The catalytic activity of tyrosinase is key to control the production of melanin, and curcumin
243 is known to reduce the production of melanin by inhibiting the activity of tyrosinase.[48-49] The
244 tyrosinase inhibitory activity assays of curcumin and CCM@ZIF-L were carried out using L-
245 DOPA as substrate.[48] Curcumin and CCM@ZIF-L were dissolved in ethanol and then diluted to
246 obtain a range of curcumin-equivalent concentrations (10, 20, 30, 40, 50 μg/mL) with PBS (0.05
247 mM, pH 6.8). For the tyrosinase inhibitory activity assay a solution of 1 mL L-DOPA (1.0 mM) in
248 PBS (0.05 mM, pH 6.8) and 0.5 mL of test sample (curcumin or CCM@ZIF-L) was incubated for
249 5 min at 37 °C while continuously agitated. Then, 0.5 mL of tyrosinase (100 Units/mL) in PBS
250 (0.05 mM, pH 6.8) was added and kept at 37 °C for 10 min while continuously agitated, after
251 which the absorbance was measured at 475 nm and the inhibition of tyrosinase activity was
252 calculated according to the following equation (4).

253 $$\text{Inhibition\%}=\left(1-\frac{A_i}{A_0}\right)\times 100\%$$

A_i represents the absorbance of the reaction mixture containing sample, while A_0 represents the absorbance of a control with no added sample.

2.12 Statistical analysis

All data are presented as mean ± standard deviation. The level of statistical significance for all tests was taken as $p < 0.05$.

3. Results and discussion

3.1 Synthesis and characterization of CCM@ZIF-L

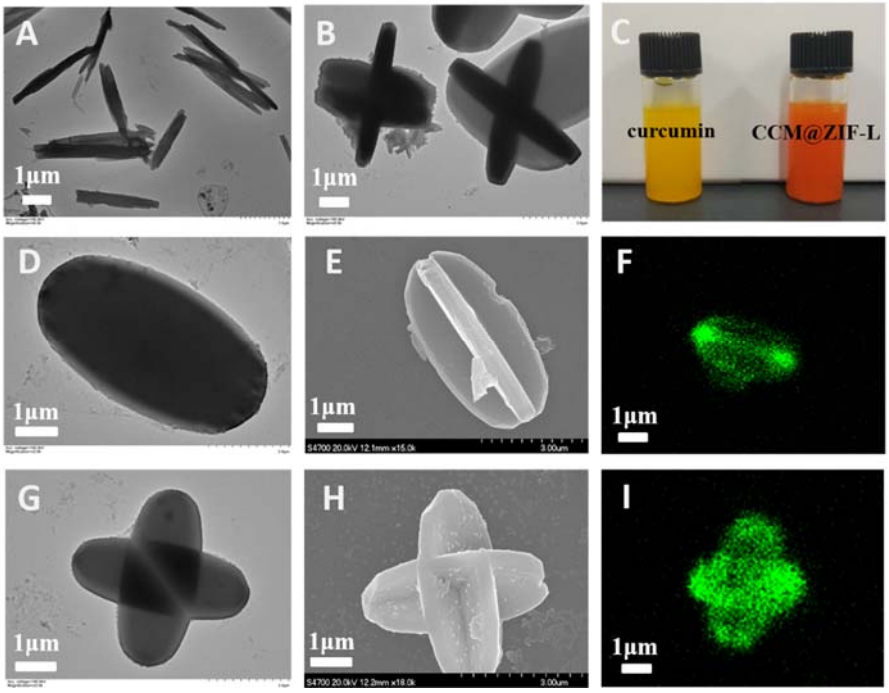

268 **Figure 1.** TEM images of microcrystals of curcumin (A) and the growing CCM@ZIF-L (B). (C)
269 Photo of curcumin in methanol stock solution (orange) and CCM@ZIF-L in deionized water (brick
270 red). TEM images of CCM@ZIF-L (D, G), SEM images of CCM@ZIF-L (E, H) and CLSM
271 images of CCM@ZIF-L (F, I).

272 The microcrystals of hydrophobic curcumin were successfully loaded into ZIF-L using an
273 antisolvent coprecipitation method to produce CCM@ZIF-L. TEM and SEM were used to
274 characterize the formation process and the morphology of CCM@ZIF-L. As the reaction time
275 increased, the stick-like microcrystals of curcumin were gradually encapsulated by ZIF-L (**Figure**
276 **1** A, B). The successful encapsulation of curcumin into ZIF-L frameworks coincided with a color
277 change from orange to brick red (**Figure 1** C). The prepared CCM@ZIF-L has a regular smooth
278 ovoid structure (**Figure 1** D, E) of which a proportion developed a cruciate flower-like structure
279 (**Figure 1** G, H), which can be ascribed as two microcrystals of curcumin assembled
280 simultaneously during the growth of CCM@ZIF-L. TEM and SEM also confirmed that the size of
281 CCM@ZIF-L is about 4 μm. The formation of CCM@ZIF-L was also observed by CLSM based
282 on the fluorescence characteristic of curcumin.[50] CCM@ZIF-L maintained the same morphology
283 and size as observed by SEM and TEM, confirming that the microcrystals of curcumin were evenly
284 encapsulated by ZIF-L (**Figure 1** F, I). The DLE of CCM@ZIF-L was determined to be 98.2%,
285 which makes ZIF-L a very suitable carrier for very hydrophobic compounds in medical
286 applications. The UV−vis spectra of CCM@ZIF-L, ZIF-L and curcumin are shown in **Figure S2**
287 A. The distinguishing absorption peaks of both curcumin and ZIF-L appeared at 428 and 213 nm
288 respectively. However, CCM@ZIF-L had the same characteristic absorption peaks as ZIF-L at
289 213 nm, indicating that curcumin was encapsulated successfully into the ZIF-L framework.
290 Curcumin, ZIF-L and CCM@ZIF-L were also characterized by means of fluorescence. The

291 characteristic fluorescence peaks of curcumin were centered at 420 nm and 550 nm, while ZIF-L
292 had an obvious peak at 440 nm (**Figure S2** B). CCM@ZIF-L had a wide peak at 565 nm, which
293 generated a small but noticeable red shift possibly due to the interaction between curcumin and
294 ZIF-L, further evidencing the incorporation of curcumin into ZIF-L. The successful encapsulation
295 of curcumin into ZIF-L was confirmed by FTIR. The characteristic peaks of ZIF-L were observed
296 at 3177, 2923 and 1566 cm^{-1} (**Figure 2** A), which correspond to aromatic C-H stretching, aliphatic
297 C-H stretching and C-N stretching of imidazole respectively.[34] The characteristic curcumin spectra
298 with bands at 3504, 1628, 1602 cm^{-1} corresponded to vibrations of free hydroxyl group of phenols,
299 C=O stretching and aromatic C=C stretching respectively.[51] Other peaks associated with curcumin
300 were observed at 1282 and 1154 cm^{-1}, attributing to aromatic C-O stretching and C-O-C stretching
301 respectively.[37] The FTIR spectrum of CCM@ZIF-L showed peaks at 3211, 2923, 1568 cm^{-1}
302 corresponding to aromatic C-H stretching, aliphatic C-H stretching and C-N stretching of
303 imidazole respectively, which are similar to the characteristic peaks of ZIF-L. The disappearance
304 of the characteristic peaks of curcumin in CCM@ZIF-L reiterated the effective encapsulation of
305 curcumin by ZIF-L. The successful construction of CCM@ZIF-L was also verified by XRD, as
306 shown in **Figure 2** B. The characteristic peaks of ZIF-L at 2θ values of 10.54, 12.80, 18.00, which
307 were obviously different from curcumin (7.98, 8.90, 15.94 and 17.12).[52] There was no change in
308 the XRD pattern of CCM@ZIF-L (10.38, 12.72 and 18.02) compared to ZIF-L, demonstrating that
309 the overall framework stability had minimum impact on its crystallinity. The zeta-potential of
310 CCM@ZIF-L was determined by DLS. The zeta potential value of CCM@ZIF-L (+4.1 mV) was
311 similar to that of ZIF-L (+3.8 mV) (**Figure 2** C), confirming that curcumin was not merely
312 adsorbed onto the surface of ZIF-L but loaded into its structure.[7]
313

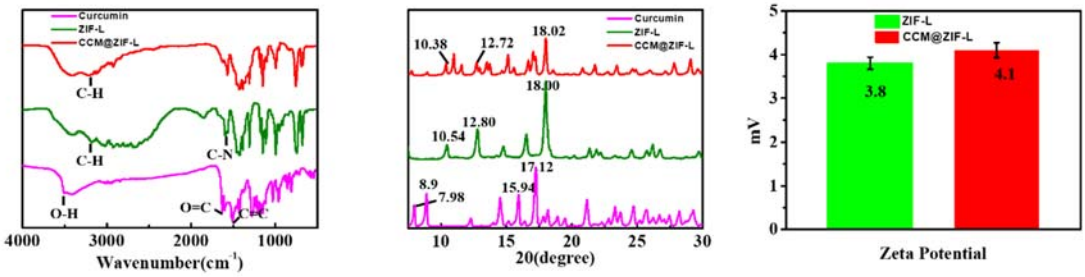

Figure 2. (A) FTIR spectra of curcumin, ZIF-L and CCM@ZIF-L. (B) XRD patterns of curcumin, ZIF-L and CCM@ZIF-L. (C) Zeta potential of ZIF-L and CCM@ZIF-L.

3.2 Stability enhancement of curcumin by ZIF-L encapsulation

Curcumin is very unstable in aqueous solution and easily hydrolyzed into smaller molecules such as ferulic acid and vanillin. Temperature, pH and light will accelerate the decomposition of curcumin in aqueous solution, however changes in the microenvironment (such as encapsulation) can improve the stability of curcumin.[53] The stability of free curcumin and CCM@ZIF-L under different environmental conditions (temperature, pH or light) were determined by monitoring the change in curcumin over time. The relative intensity of CCM@ZIF-L is about 5 times than that of free curcumin after thermal treatment for 4 h (Figure 3A), signifying that the encapsulation of ZIF-L improved the temperature stability of curcumin. When the pH value increased from 5.4 to 8.4. the relative intensity of free curcumin gradually decreased (**Figure 3**B), while the relative intensity of CCM@ZIF-L gradually decreased without significant change. Due to the protective effect of ZIF-L, CCM@ZIF-L exhibited higher pH stability than free curcumin in an aqueous environment. The relative intensity of CCM@ZIF-L is about 3 times that of free curcumin after 4 hours in **Figure 3**C. Thus, ZIF-L could efficiently protect curcumin by avoiding photodegradation. Moreover, the stability enhancement of CCM@ZIF-L was further supported by the change of relative intensity with time under different conditions (temperature, pH or light) in **Figure S3-5.**

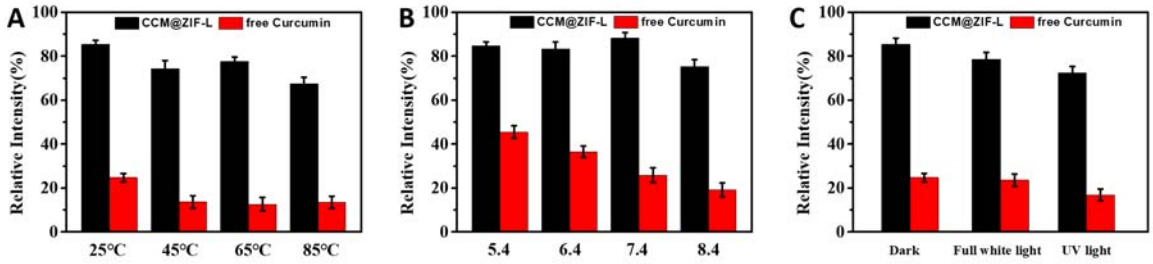

Figure 3. Stability of free curcumin and CCM@ZIF-L in PBS solution at different temperatures (A), pH (B) or light (C) after 4 h.

3.3 pH-responsive release of curcumin from CCM@ZIF-L

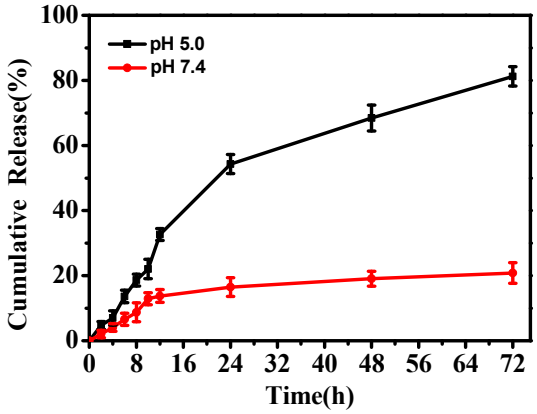

Figure 4. The *in vitro* pH-response release profiles of curcumin from CCM@ZIF-L at different pH (pH 5.0 or 7.4) in PBS containing 1 wt % of Tween-80.

The pH-responsive release of curcumin from CCM@ZIF-L was investigated in an *in vitro* drug release experiment, which was carried out in PBS solution at different pH conditions (pH 5.0 or 7.4).[30] Meanwhile, the addition of Tween-80 (1 wt%, PBS) was used to improve the stability of free curcumin, providing an excellent monitoring condition for drug released from CCM@ZIF-L in an aqueous environment.[37] pH 5.0 was chosen to simulate the acidic condition in tumor cells, while pH 7.4 represents the physiological pH. The cumulative drug release of CCM@ZIF-L reached to 81.2 % after 72 h at pH 5.0. In comparison only 20.8 % of curcumin was released after

72 h in PBS at pH 7.4 (Figure 4), indicating that CCM@ZIF-L CCM@ZIF-L achieved pH-responsive release. Therefore, the controlled drug release behavior could be exploited to enhance cytotoxicity toward tumor cells.[54-55]

3.4 *In vitro* cytotoxicity study

The anticancer activity of curcumin and CCM@ZIF-L against A549 cells was investigated through *in vitro* cytotoxicity experiments. Prior to undertaking the *in vitro* cytotoxicity experiments, we evaluated the biocompatibility of ZIF-L in A549 cells At ZIF-L concentrations below 50 μg/mL all of cell survival rates exceed 80 % (Figure 5A), indicating that ZIF-L has good biocompatibility and is suitable as a safe drug carrier for cancer therapy. As the curcumin concentration (free and encapsulated) increased from 1 to 5 μg/mL, the viability of A549 cells decreased (Figure 5B) More specifically, CCM@ZIF-L showed the lower viability with regards to A549 cells than free curcumin at the same concentration. CCM@ZIF-L induced almost 48.2 % of cell death against A549 cells compared to only 4.9 % cell death caused by curcumin at the equivalent concentration of 2 μg/ml. The cytotoxicity was more pronounced at higher concentration, CCM@ZIF-L induced 81 % decrease in cell viability compared to a 20 % decrease in cell viability by free curcumin at the equivalent concentration of 5 μg/ml. The significant improvement of the cytotoxicity of CCM@ZIF-L on A549 cells can be attributed to the protective encapsulation of ZIF-L and the effective sustainable drug release. According to the result of stability experiment, free curcumin would sharp degrade in short time. However, CCM@ZIF-L showed the excellent stability due to the ZIF-L encapsulation. Additionally, CCM@ZIF-L achieved the effective sustainable release of curcumin for a long time in acidic cancer cells environment. In summary, the results of cytotoxicity assay indicated clearly that the CCM@ZIF-L displayed obvious inhibition effects on cell proliferation.[56]

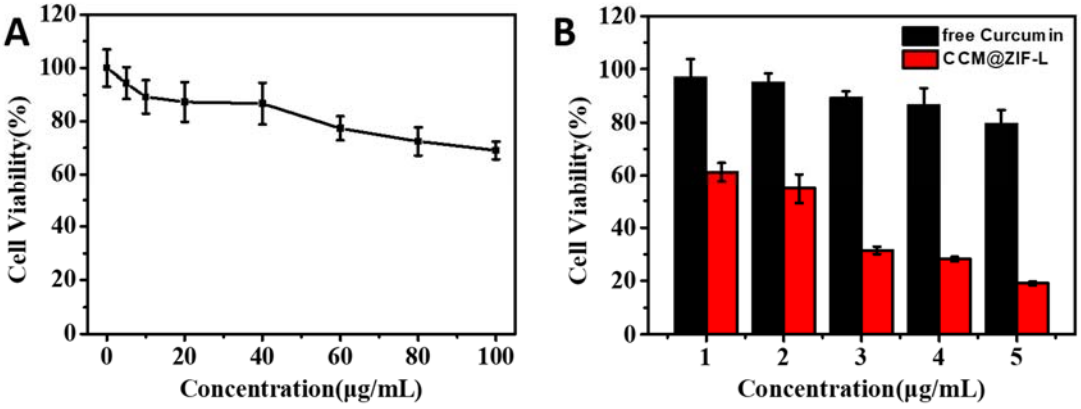

Figure 5. (A) *In vitro* biocompatibility of ZIF-L against A549 cells. (B) *In vitro* cytotoxicity of free curcumin and CCM@ZIF-L against A549 cells at different concentrations for 72 h.

3.5 Cellular uptake of encapsulated curcumin

The effective internalization of drugs into cancer cells would be a crucially important process for any cancer treatment.[41] The cellular uptake of curcumin and CCM@ZIF-L on A549 cells was investigated by employing CLSM. The uni-laminar A549 cells were incubated with free curcumin and CCM@ZIF-L at the equivalent drug concentration of 5 μg/ml for 4 h. For comparison, A549 cells were also treated with DMSO instead of drug as a control treatment. The commercial fluorescent dye PI was used to characterize morphology of cell, and the green fluorescence of curcumin indicated the drug distribution in cells. As shown in **Figure 6**, the red fluorescent intensity of CCM@ZIF-L was similar to that of free curcumin. In contrast, CCM@ZIF-L showed significantly stronger green fluorescence intensity than free curcumin, indicating that A549 cells displayed higher accumulations of curcumin than cells treated with free curcumin. According to the stability experiment, ZIF-L encapsulated curcumin was stable under physiological conditions and the pH-responsive behavior made curcumin release around cancer cell. The positive zeta potential of CCM@ZIF-L (Figure 2C) can promote the electrostatic interactions with cellular membranes (with negative potential).[57] Hence, curcumin can be released in close proximity of

388 cancer cell membrane and readily taken up by cancer cells. In short, ZIF-L could be used as an
389 efficient safe carrier to protect curcumin against degradation and enhance the bioavailability of
390 curcumin by effective cellular internalization.

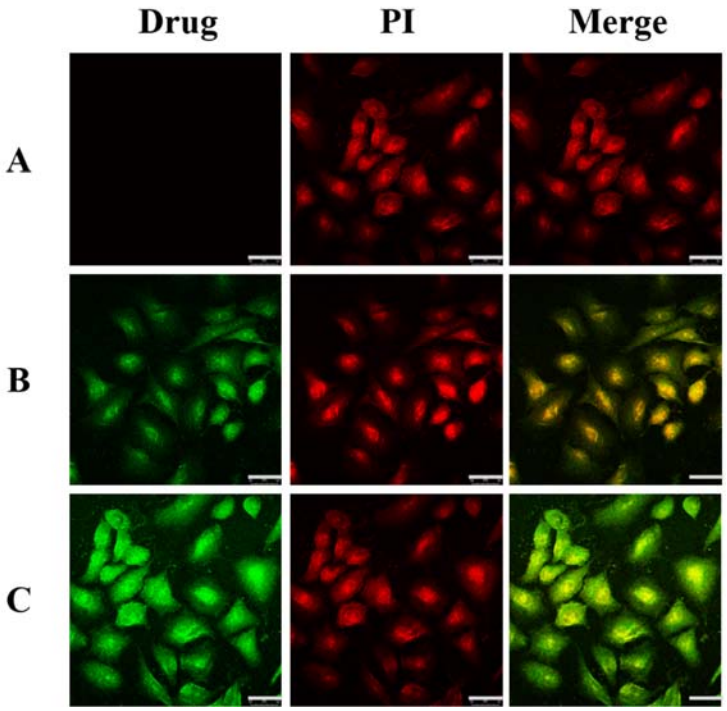

391

392 **Figure 6.** CLSM images on A549 cells incubated with DMSO (A), free curcumin (B) and
393 CCM@ZIF-L (C) at the equivalent curcumin concentration (5 μg/mL) for 4 h, respectively. Each
394 series can be classified to the cell nucleus (red fluorescence, stained by PI), free curcumin or
395 CCM@ZIF-L (green fluorescence); all scale bars are 20 μm.

396 **3.6 Cellular Anti-oxidant Activity**

397 Previous studies have shown that curcumin has significant antioxidant activity.[58] To verify
398 the effect of encapsulation on the antioxidant activity of curcumin, MGC-803 cells were chosen
399 as an oxidative cell model to assess the cellular antioxidant activity (CAA) of free curcumin and
400 encapsulated curcumin (CCM@ZIF-L). In keeping with the CAA principles[45], peroxy radicals
401 produced by ABAP could cause the oxidation of DCFH to form the fluorescent DCF. The

402 subsequent DCF fluorescence intensity would then be representative of the magnitude of the
403 cellular oxidation damage caused by the presence of free radicals. Along the same vein, the
404 antioxidant capacity of any antioxidant could be reflected by the reduced DCF fluorescence
405 intensity. CCM@ZIF-L showed the highest free radical scavenging capacity in MGC 803 cells
406 compared to free curcumin or ZIF-L (**Figure 7**A). The CAA value can be calculated according to
407 equation (3). The CAA value of CCM@ZIF-L (69.8) was higher than free curcumin (31.4) and
408 ZIF-L (10.9) (Figure 7B), indicating that the cellular anti-oxidant activity of curcumin was
409 enhanced by the encapsulation of curcumin in ZIF-L. Moreover, it was confirmed again that
410 ZIF-L can significantly enhance cell internalization and improve bioavailability of hydrophobic
411 drugs.

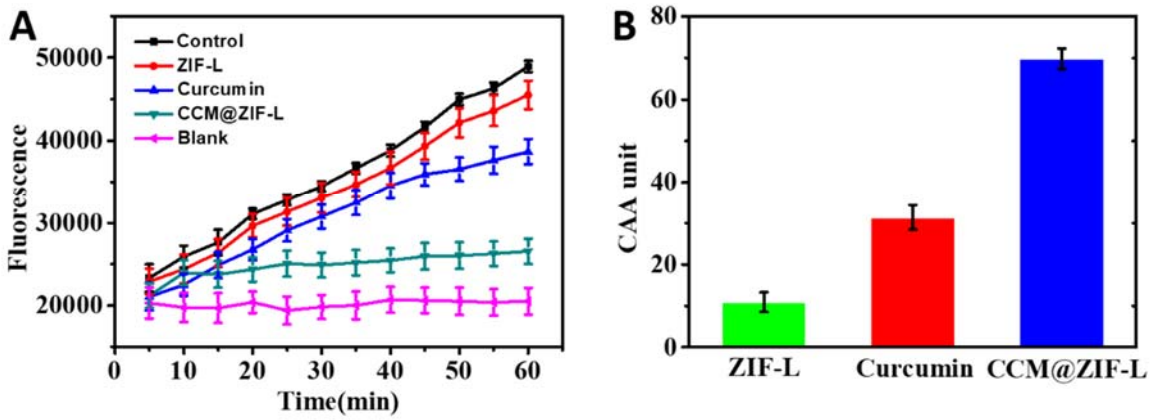

412

413 **Figure 7.** Cellular antioxidant activity of curcumin and CCM@ZIF-L. (A) The kinetics curve of
414 DCF fluorescence from cellular antioxidant activity (CAA) of free curcumin, ZIF-L, CCM@ZIF-
415 L, control, and blank sample. (B) Cellular antioxidant activity values of different nanoparticles.

416 **3.7 Tyrosinase inhibitory activity**

417 The catalytic activity of tyrosinase is the key to control the production of melanin, and
418 curcumin is known to reduce the production of melanin by inhibiting the activity of tyrosinase.[48]

The tyrosinase inhibitory activity of curcumin and CCM@ZIF-L was examined *in vitro*. The inhibition percentage of curcumin and CCM@ZIF-L was enhanced with the increase of concentration among the evaluated range. The inhibition of tyrosinase by free curcumin at 0.5 μg/ml was found to be 6.5 %, which increased to 36.5 % when the concentration of curcumin was increased ten-fold to 5 μg/ml (Figure S6). In comparison, the antioxidant scavenging capacity of CCM@ZIF-L at 0.5 μg/ml was found to be 29.7 %. Hence, curcumin encapsulated in ZIF-L (CCM@ZIF-L) facilitated a much more effective anti-tyrosinase activity compared to free curcumin at the same concentration. This improvement may be due to the enhanced dispersibility and stability of curcumin in aqueous solution after ZIF-L encapsulation.

4. Conclusion

In summary, we proposed a synthesis process of encapsulating insoluble drugs with ZIF-L by the antisolvent coprecipitation method. The prepared CCM@ZIF-L possessed high DLE (98.21 %) and the regular leaf or cruciate flower-like structure. The results of SEM, TEM, CLSM, FTIR, XRD and zeta-potential suggested the great encapsulation of curcumin was achieved by ZIF-L. CCM@ZIF-L showed superior stability to free curcumin under different temperatures, pH or light conditions due to the protective encapsulation of ZIF-L. *In vitro* drug release results revealed an 81.2 % drug release a 72 h period in simulated tumor acidic conditions, implying that CCM@ZIF-L performed the pH-sensitive release behavior. Cytotoxicity and cellular internalization results showed enhanced anticancer activity of CCM@ZIF-L against A549 cells. Moreover, the cellular antioxidant activity of ZIF-L loaded curcumin was significantly improved than free curcumin on MGC-803 cells. Therefore, our pH-sensitive drug delivery system based on the microcrystal of an

insoluble drug provided a promising potential in cancer treatment for broadening the applications of MOF in biomedical field.

AUTHOR INFORMATION

Corresponding Author

* E-mail: FVriesekoop@harper-adams.ac.uk

* E-mail: lianghao@mail.buct.edu.cn

Author Contributions

The first two authors have equal contributions

Notes

The authors declare no competing financial interest.

ACKNOWLEDGMENT

The authors acknowledged financial support from the National Natural Science Foundation of China (21878014), the Beijing Natural Science Foundation-Beijing Municipal Education Commission Joint Funding project (KZ201710020014), the Double First-rate Program (ylkxj03) and the 111 Project (B13005).

REFERENCES

1. Zheng, H.; Zhang, Y.; Liu, L.; Wan, W.; Guo, P.; Nystrom, A. M.; Zou, X., One-pot Synthesis of Metal-Organic Frameworks with Encapsulated Target Molecules and Their Applications for Controlled Drug Delivery. *J Am Chem Soc* **2016,** *138* (3), 962-8.

2.Wang, C.; Xu, L.; Liang, C.; Xiang, J.; Peng, R.; Liu, Z., Immunological responses triggered by photothermal therapy with carbon nanotubes in combination with anti-CTLA-4 therapy to inhibit cancer metastasis. *Adv Mater* **2014,** *26* (48), 8154-62.

3.Tiloke, C.; Anand, K.; Gengan, R. M.; Chuturgoon, A. A., Moringa oleifera and their phytonanoparticles: Potential antiproliferative agents against cancer. *Biomed Pharmacother* **2018,** *108*, 457-466.

4.Safe, S.; Kasiappan, R., Natural Products as Mechanism-based Anticancer Agents: Sp Transcription Factors as Targets. *Phytother Res* **2016,** *30* (11), 1723-1732.

5.Li, W.; Zhang, L.; Ge, X.; Xu, B.; Zhang, W.; Qu, L.; Choi, C. H.; Xu, J.; Zhang, A.; Lee, H.; Weitz, D. A., Microfluidic fabrication of microparticles for biomedical applications. *Chem Soc Rev* **2018,** *47* (15), 5646-5683.

6.Ferrari, R.; Sponchioni, M.; Morbidelli, M.; Moscatelli, D., Polymer nanoparticles for the intravenous delivery of anticancer drugs: the checkpoints on the road from the synthesis to clinical translation. *Nanoscale* **2018**.

7.Pan, Q. S.; Chen, T. T.; Nie, C. P.; Yi, J. T.; Liu, C.; Hu, Y. L.; Chu, X., In Situ Synthesis of Ultrathin ZIF-8 Film-Coated MSNs for Codelivering Bcl 2 siRNA and Doxorubicin to Enhance Chemotherapeutic Efficacy in Drug-Resistant Cancer Cells. *ACS Appl Mater Interfaces* **2018,** *10* (39), 33070-33077.

8.He, M. N.; Zhou, J. J.; Chen, J.; Zheng, F. C.; Wang, D. D.; Shi, R. H.; Guo, Z.; Wang, H. B.; Chen, Q. W., Fe_3O_4@carbon@zeolitic imidazolate framework-8 nanoparticles as multifunctional pH-responsive drug delivery vehicles for tumor therapy in vivo. *J Mater Chem B* **2015,** *3* (46), 9033-9042.

9.Chowdhuri, A. R.; Laha, D.; Pal, S.; Karmakar, P.; Sahu, S. K., One-pot synthesis of folic acid encapsulated upconversion nanoscale metal organic frameworks for targeting, imaging and pH responsive drug release. *Dalton Trans* **2016,** *45* (45), 18120-18132.

10.Hu, Y.; Wu, S.; He, Y.; Deng, L., A redox prodrug micelle co-delivering camptothecin and curcumin for synergetic B16 melanoma cells inhibition. *Chem Eng J* **2019,** *362*, 877-886.

11.Niu, S.; Williams, G. R.; Wu, J.; Wu, J.; Zhang, X.; Zheng, H.; Li, S.; Zhu, L.-M., A novel chitosan-based nanomedicine for multi-drug resistant breast cancer therapy. *Chem Eng J* **2019,** *369*, 134-149.

12.Ma, Y.; Shi, L.; Liu, F.; Zhang, Y.; Pang, Y.; Shen, X., Self-assembled thixotropic silver cluster hydrogel for anticancer drug release. *Chem Eng J* **2019,** *362*, 650-657.

13.Gong, P.; Ji, S.; Wang, J.; Dai, D.; Wang, F.; Tian, M.; Zhang, L.; Guo, F.; Liu, Z., Fluorescence-switchable ultrasmall fluorinated graphene oxide with high near-infrared absorption for controlled and targeted drug delivery. *Chem Eng J* **2018,** *348*, 438-446.

14.Zhang, J.; Li, S.; Ju, D.-D.; Li, X.; Zhang, J.-C.; Yan, X.; Long, Y.-Z.; Song, F., Flexible inorganic core-shell nanofibers endowed with tunable multicolor upconversion fluorescence for simultaneous monitoring dual drug delivery. *Chem Eng J* **2018,** *349*, 554-561.

15.Liu, F.; Huang, P.; Huang, D.; Liu, S.; Cao, Q.; Dong, X.; Zhang, H.; Ko, F.; Zhou, W., Smart "on-off" responsive drug delivery nanosystems for potential imaging diagnosis and targeted tumor therapy. *Chem Eng J* **2019,** *365*, 358-368.

16.Babikova, D.; Kalinova, R.; Momekova, D.; Ugrinova, I.; Momekov, G.; Dimitrov, I., Multifunctional Polymer Nanocarrier for Efficient Targeted Cellular and Subcellular Anticancer Drug Delivery. *ACS Biomaterials Science & Engineering* **2019,** *5* (5), 2271-2283.

17.Kirchon, A.; Feng, L.; Drake, H. F.; Joseph, E. A.; Zhou, H. C., From fundamentals to applications: a toolbox for robust and multifunctional MOF materials. *Chem Soc Rev* **2018,** *47* (23), 8611-8638.

18.Wu, Q.; Niu, M.; Chen, X.; Tan, L.; Fu, C.; Ren, X.; Ren, J.; Li, L.; Xu, K.; Zhong, H.; Meng, X., Biocompatible and biodegradable zeolitic imidazolate framework/polydopamine nanocarriers for dual stimulus triggered tumor thermo-chemotherapy. *Biomaterials* **2018,** *162*, 132-143.

19.Yan, L.; Chen, X.; Wang, Z.; Zhang, X.; Zhu, X.; Zhou, M.; Chen, W.; Huang, L.; Roy, V. A. L.; Yu, P. K. N.; Zhu, G.; Zhang, W., Size Controllable and Surface Tunable Zeolitic Imidazolate Framework-8-Poly(acrylic acid sodium salt) Nanocomposites for pH Responsive Drug Release and Enhanced in Vivo Cancer Treatment. *ACS Appl Mater Interfaces* **2017,** *9* (38), 32990-33000.

20.Soltani, B.; Nabipour, H.; Nasab, N. A., Efficient Storage of Gentamicin in Nanoscale Zeolitic Imidazolate Framework-8 Nanocarrier for pH-Responsive Drug Release. *J Inorg Organomet P* **2018,** *28* (3), 1090-1097.

21.Duan, C.; Zhang, H.; Li, F.; Xiao, J.; Luo, S.; Xi, H., Hierarchically porous metal-organic frameworks: rapid synthesis and enhanced gas storage. *Soft Matter* **2018,** *14* (47), 9589-9598.

22.Chen, X.; Niu, T.; Gao, Y.; Liang, X.; Li, S.; Zhang, L.; Li, L.; Wang, T.; Su, Z.; Wang, C., Tunable synthesis of pH-responsive biodegradable ZnO nanospheres assembled from ultrasmall particles for cancer chemotherapy. *Chem. Eng. J* **2019,** *371*, 443-451.

23.Guo, J.; Suma, T.; Richardson, J. J.; Ejima, H., Modular Assembly of Biomaterials Using Polyphenols as Building Blocks. *ACS Biomaterials Science & Engineering* **2019**.

24.Zheng, B.; Peng, S.; Zhang, X.; McClements, D. J., Impact of Delivery System Type on Curcumin Bioaccessibility: Comparison of Curcumin-Loaded Nanoemulsions with Commercial Curcumin Supplements. *J Agric Food Chem* **2018,** *66* (41), 10816-10826.

25.Liedana, N.; Galve, A.; Rubio, C.; Tellez, C.; Coronas, J., CAF@ZIF-8: one-step encapsulation of caffeine in MOF. *ACS Appl Mater Interfaces* **2012,** *4* (9), 5016-21.

26.Gomar, M.; Yeganegi, S. J. M.; Materials, M., Corrigendum to "Adsorption of 5-fluorouracil, hydroxyurea and mercaptopurine drugs on zeolitic imidazolate frameworks (ZIF-7, ZIF-8 and ZIF-9)". Microporous Mesoporous Mater **2018,** *258*, 277-280.

27.Song, M.-R.; Li, D.-Y.; Nian, F.-Y.; Xue, J.-P.; Chen, J.-J., Zeolitic imidazolate metal organic framework-8 as an efficient pH-controlled delivery vehicle for zinc phthalocyanine in photodynamic therapy. *Journal of Materials Science* **2017,** *53* (4), 2351-2361.

28.Shi, Z.; Chen, X.; Zhang, L.; Ding, S.; Wang, X.; Lei, Q.; Fang, W., FA-PEG decorated MOF nanoparticles as a targeted drug delivery system for controlled release of an autophagy inhibitor. *Biomater Sci* **2018,** *6* (10), 2582-2590.

29.Zhuang, J.; Kuo, C. H.; Chou, L. Y.; Liu, D. Y.; Weerapana, E.; Tsung, C. K., Optimized metal-organic-framework nanospheres for drug delivery: evaluation of small-molecule encapsulation. *ACS Nano* **2014,** *8* (3), 2812-9.

30.Yang, J. C.; Chen, Y.; Li, Y. H.; Yin, X. B., Magnetic Resonance Imaging-Guided Multi-Drug Chemotherapy and Photothermal Synergistic Therapy with pH and NIR-Stimulation Release. *ACS Appl Mater Interfaces* **2017,** *9* (27), 22278-22288.

31.Jiang, W.; Zhang, H.; Wu, J.; Zhai, G.; Li, Z.; Luan, Y.; Garg, S., CuS@MOF-Based Well-Designed Quercetin Delivery System for Chemo-Photothermal Therapy. *ACS Appl Mater Interfaces* **2018,** *10* (40), 34513-34523.

32.Vasconcelos, I. B.; Silva, T. G. d.; Militão, G. C. G.; Soares, T. A.; Rodrigues, N. M.; Rodrigues, M. O.; Costa, N. B. d.; Freire, R. O.; Junior, S. A., Cytotoxicity and slow release of the anti-cancer drug doxorubicin from ZIF-8. *RSC Advances* **2012,** *2* (25).

33.Shu, F.; Lv, D.; Song, X.-L.; Huang, B.; Wang, C.; Yu, Y.; Zhao, S.-C., Fabrication of a hyaluronic acid conjugated metal organic framework for targeted drug delivery and magnetic resonance imaging. *RSC Advances* **2018,** *8* (12), 6581-6589.

34.Mao, H.; Zhen, H.-G.; Ahmad, A.; Li, S.-H.; Liang, Y.; Ding, J.-F.; Wu, Y.; Li, L.-Z.; Zhao, Z.-P., Highly selective and robust PDMS mixed matrix membranes by embedding two-dimensional ZIF-L for alcohol permselective pervaporation. *Journal of Membrane Science* **2019,** *582*, 307-321.

35. Prabhu, R., Mohammed, M.A., Anjali, R., Archunan, G., Prabhu, N.M., Pugazhendhi, A. and Suganthy, N., 2019. Ecofriendly one pot fabrication of methyl gallate@ ZIF-L nanoscale hybrid as pH responsive drug delivery system for lung cancer therapy. *Process Biochemistry*. **2019,** *84*, 39-52.

36.Wang, L.; Guan, H.; Wang, Z.; Xing, Y.; Zhang, J.; Cai, K., Hybrid Mesoporous-Microporous Nanocarriers for Overcoming Multidrug Resistance by Sequential Drug Delivery. *Mol Pharm* **2018,** *15* (7), 2503-2512.

37.Zheng, M.; Liu, S.; Guan, X.; Xie, Z., One-Step Synthesis of Nanoscale Zeolitic Imidazolate Frameworks with High Curcumin Loading for Treatment of Cervical Cancer. *ACS Appl Mater Interfaces* **2015,** *7* (40), 22181-7.

38.Malekmohammadi, S.; Hadadzadeh, H.; Farrokhpour, H.; Amirghofran, Z., Immobilization of gold nanoparticles on folate-conjugated dendritic mesoporous silica-coated reduced graphene oxide nanosheets: a new nanoplatform for curcumin pH-controlled and targeted delivery. *Soft Matter* **2018,** *14* (12), 2400-2410.

39.Xiang, Y.; Duan, X.; Feng, L.; Jiang, S.; Deng, L.; Shen, J.; Yang, Y.; Guo, R., tLyp-1-conjugated GSH-sensitive biodegradable micelles mediate enhanced pUNO1-hTRAILa/curcumin co-delivery to gliomas. *Chem. Eng. J* **2019,** *374*, 392-404.

40.Su, C.-Y.; Liu, J.-J.; Ho, Y.-S.; Huang, Y.-Y.; Chang, V. H.-S.; Liu, D.-Z.; Chen, L.-C.; Ho, H.-O.; Sheu, M.-T., Development and characterization of docetaxel-loaded lecithin-stabilized micellar drug delivery system (L sb MDDs) for improving the therapeutic efficacy and reducing systemic toxicity. *European Journal of Pharmaceutics and Biopharmaceutics* **2018,** *123*, 9-19.

41.Zhang, H.; Jiang, W.; Liu, R.; Zhang, J.; Zhang, D.; Li, Z.; Luan, Y., Rational Design of Metal Organic Framework Nanocarrier-Based Codelivery System of Doxorubicin

Hydrochloride/Verapamil Hydrochloride for Overcoming Multidrug Resistance with Efficient Targeted Cancer Therapy. *ACS Appl Mater Interfaces* **2017,** *9* (23), 19687-19697.

42.Li, Y.; Xu, N.; Zhu, W.; Wang, L.; Liu, B.; Zhang, J.; Xie, Z.; Liu, W., Nanoscale Melittin@Zeolitic Imidazolate Frameworks for Enhanced Anticancer Activity and Mechanism Analysis. *ACS Appl Mater Interfaces* **2018,** *10* (27), 22974-22984.

43.Chen, X.; Tong, R.; Shi, Z.; Yang, B.; Liu, H.; Ding, S.; Wang, X.; Lei, Q.; Wu, J.; Fang, W., MOF Nanoparticles with Encapsulated Autophagy Inhibitor in Controlled Drug Delivery System for Antitumor. *ACS Appl Mater Interfaces* **2018,** *10* (3), 2328-2337.

44.Cai, W.; Gao, H.; Chu, C.; Wang, X.; Wang, J.; Zhang, P.; Lin, G.; Li, W.; Liu, G.; Chen, X., Engineering Phototheranostic Nanoscale Metal-Organic Frameworks for Multimodal Imaging-Guided Cancer Therapy. *ACS Appl Mater Interfaces* **2017,** *9* (3), 2040-2051.

45.Wolfe, K. L.; Liu, R. H., Cellular antioxidant activity (CAA) assay for assessing antioxidants, foods, and dietary supplements. *J Agric Food Chem* **2007,** *55* (22), 8896-907.

46.Fan, Y.; Liu, Y.; Gao, L.; Zhang, Y.; Yi, J., Improved chemical stability and cellular antioxidant activity of resveratrol in zein nanoparticle with bovine serum albumin-caffeic acid conjugate. *Food Chem* **2018,** *261*, 283-291.

47.Zhao, C.; She, T.; Wang, L.; Su, Y.; Qu, L.; Gao, Y.; Xu, S.; Cai, S.; Shou, C., Daucosterol inhibits cancer cell proliferation by inducing autophagy through reactive oxygen species-dependent manner. *Life Sci* **2015,** *137*, 37-43.

48.Wei, Y.; Zhang, J.; Zhou, Y.; Bei, W.; Li, Y.; Yuan, Q.; Liang, H., Characterization of glabridin/hydroxypropyl-beta-cyclodextrin inclusion complex with robust solubility and enhanced bioactivity. *Carbohydr Polym* **2017,** *159*, 152-160.

49.Van Tran, V.; Loi Nguyen, T.; Moon, J.-Y.; Lee, Y.-C., Core-shell materials, lipid particles and nanoemulsions, for delivery of active anti-oxidants in cosmetics applications: challenges and development strategies. *Chemical Engineering Journal* **2019,** *368*, 88-114.

50.Masek, A.; Chrzescijanska, E.; Zaborski, M. J. E. A., Characteristics of curcumin using cyclic voltammetry, UV–vis, fluorescence and thermogravimetric analysis. **2013,** *107* (107), 441-447.

51.Sahne, F.; Mohammadi, M.; Najafpour, G. D., Single-Layer Assembly of Multifunctional Carboxymethylcellulose on Graphene Oxide Nanoparticles for Improving in Vivo Curcumin Delivery into Tumor Cells. *ACS Biomaterials Science & Engineering* **2019,** *5* (5), 2595-2609.

52.Wu, J.; Wang, J.; Zhang, J.; Zheng, Z.; Kaplan, D. L.; Li, G.; Wang, X., Oral Delivery of Curcumin Using Silk Nano- and Microparticles. *ACS Biomaterials Science & Engineering* **2018,** *4* (11), 3885-3894.

53.Hanne Hjorth Tønnesen a, Ma´r Ma´sson b, Thorsteinn Loftsson b, Studies of curcumin and curcuminoids. XXVII. Cyclodextrin complexation: solubility, chemical and photochemical stability. *International Journal of Pharmaceutics* **2002,** *244*, 127-135.

54.Tian, Z.; Yao, X.; Ma, K.; Niu, X.; Grothe, J.; Xu, Q.; Liu, L.; Kaskel, S.; Zhu, Y., Metal-Organic Framework/Graphene Quantum Dot Nanoparticles Used for Synergistic Chemo- and Photothermal Therapy. *ACS Omega* **2017,** *2* (3), 1249-1258.

55.Chen, R.; Zhang, J.; Wang, Y.; Chen, X.; Zapien, J. A.; Lee, C. S., Graphitic carbon nitride nanosheet@metal-organic framework core-shell nanoparticles for photo-chemo combination therapy. *Nanoscale* **2015,** *7* (41), 17299-305.

56.Yang, K.; Yang, K.; Chao, S.; Wen, J.; Pei, Y.; Pei, Z., A supramolecular hybrid material constructed from pillar[6]arene-based host-guest complexation and ZIF-8 for targeted drug delivery. *Chem Commun (Camb)* **2018,** *54* (70), 9817-9820.

57.Tiwari, A.; Singh, A.; Garg, N.; Randhawa, J. K., Curcumin encapsulated zeolitic imidazolate frameworks as stimuli responsive drug delivery system and their interaction with biomimetic environment. *Sci Rep* **2017,** *7* (1), 12598.

58.Mahmood, K.; Zia, K. M.; Zuber, M.; Tabasum, S.; Rehman, S.; Zia, F.; Noreen, A., Morphological and thermal studies of chitin-curcumin blends derived polyurethanes. *Int J Biol Macromol* **2017,** *105* (Pt 1), 1180-1191.

Supporting Information

Crystal seeded growth of pH-responsive metal-organic framework for enhancing encapsulation, stability and bioactivity of hydrophobicity compounds

Zexun Liu,[†] Qiao Wu,[†] Jie He,[†] Frank Vriesekoop,[‡,*] and Hao Liang[†,*]

[†] State Key Laboratory of Chemical Resource Engineering, Beijing University of Chemical Technology, Beijing100029, P. R. China

[‡] Department of Food Technology and Innovation, Harper Adams University, Newport TF10 8NB, Shropshire, England

Corresponding Author

* E-mail: FVriesekoop@harper-adams.ac.uk

* E-mail: lianghao@mail.buct.edu.cn

Supplementary figures

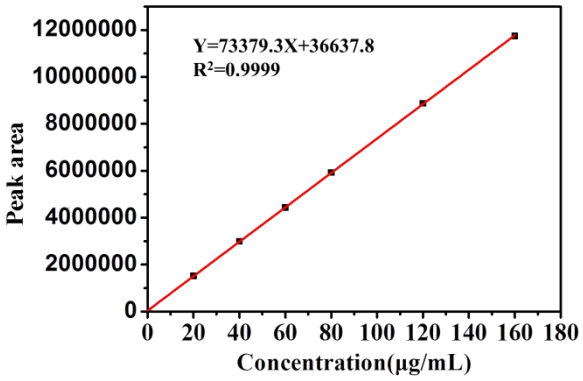

Fig.S1 Standard curve of curcumin

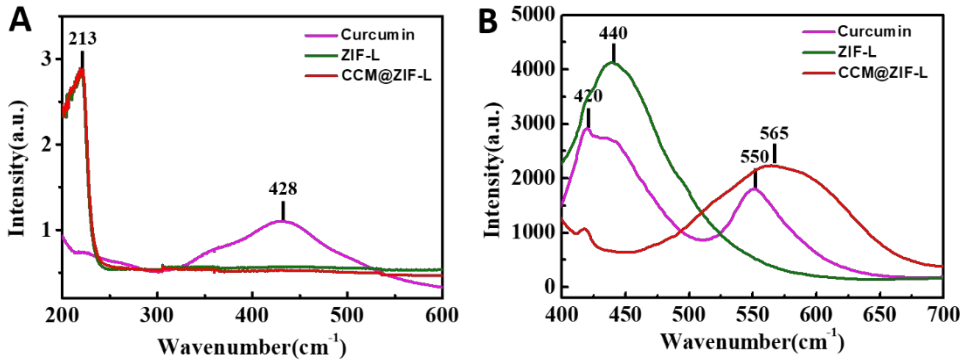

Fig.S2 (A) The UV−vis absorption of curcumin, ZIF-L and CCM@ZIF-L. (B) The fluorescence spectra of curcumin, ZIF-L and CCM@ZIF-L under the excitation of blue light (445−490 nm).

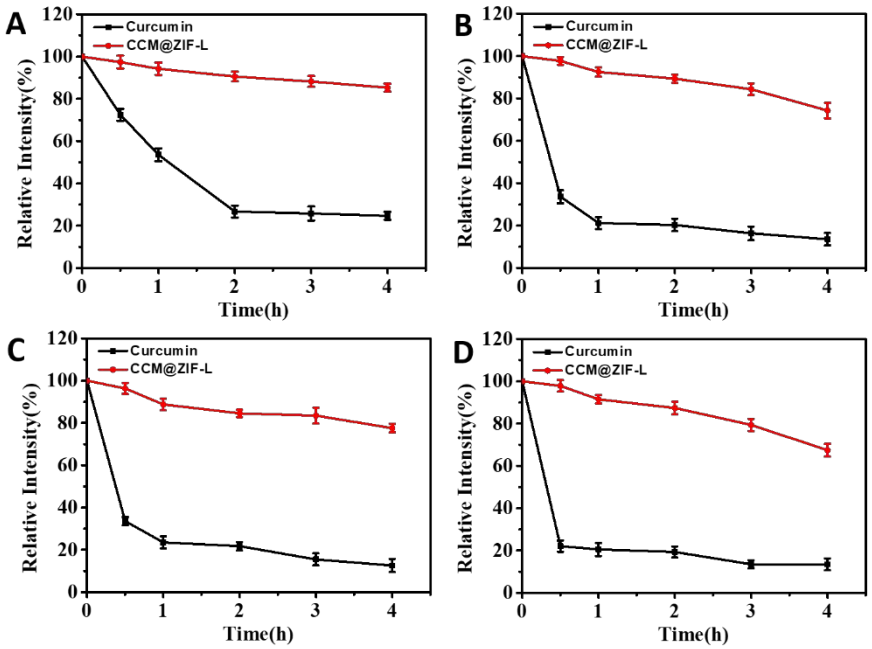

Fig.S3 Stability of free curcumin and CCM@ZIF-L in PBS solution at a range of temperatures. (A) for 4 h at 25 °C, (B) for 4 h at 45 °C, (C) for 4 h at 65 °C, and (D) for 4 h at 85 °C.

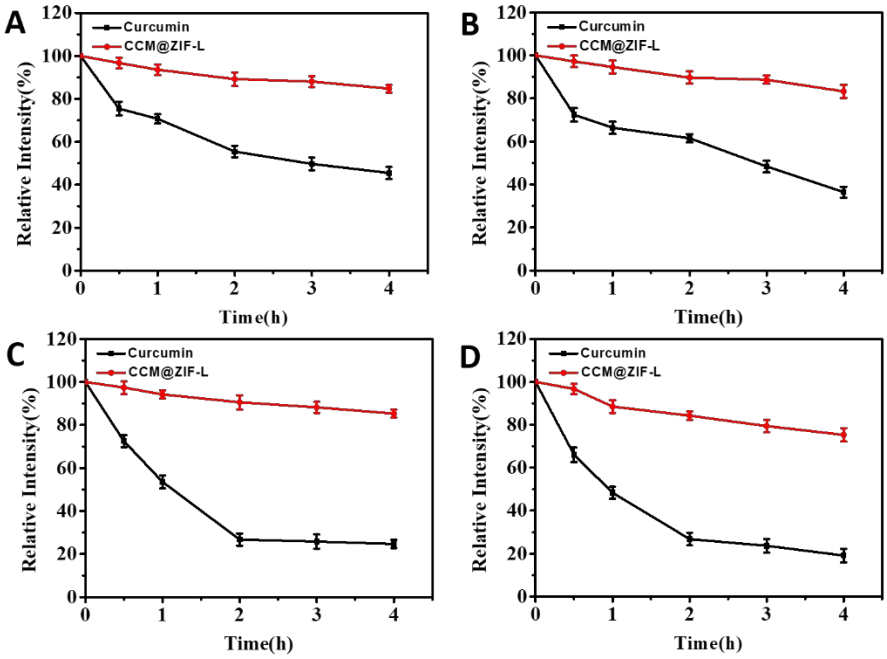

Fig.S4 Stability of free curcumin and CCM@ZIF-L in PBS solution at a range of pHs. (A) at pH 5.4, (B) pH 6.4, (C) pH 7.4, and (D) pH 8.4 for 4 h

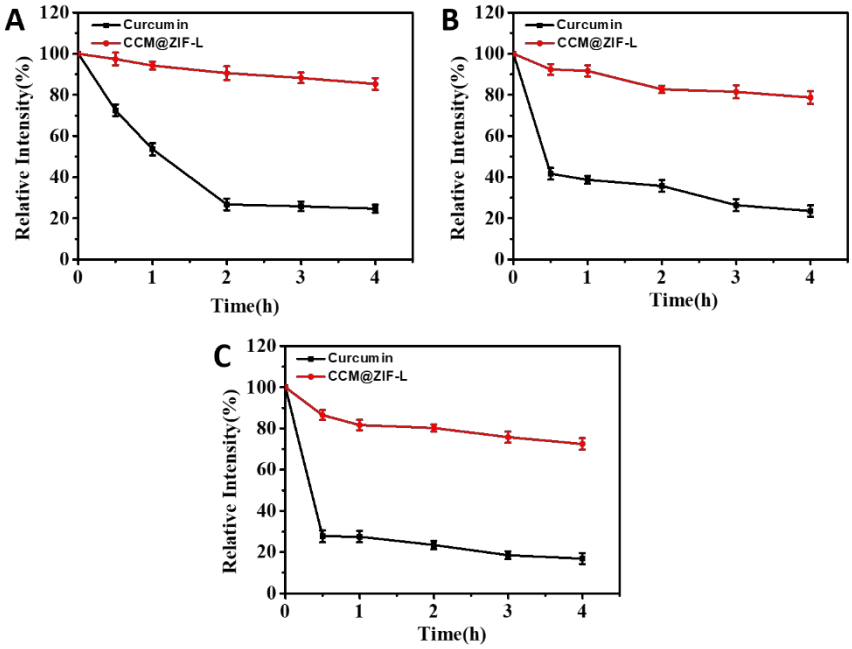

Fig.S5 Stability of free curcumin and CCM@ZIF-L in PBS solution at different light source exposures. (A) At dark, (B) in full white light, and (C) exposed to UV light for 4 h.

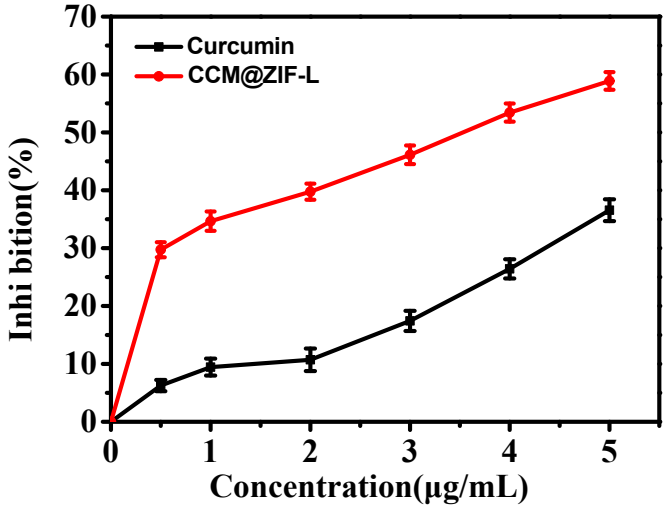

Fig.S6 Comparative tyrosinase inhibition activities of curcumin and CCM@ZIF-L.